Designing a Measuring Campaign for Axial Flux Permanent Magnet Generators of Small-Scale Wind Turbines

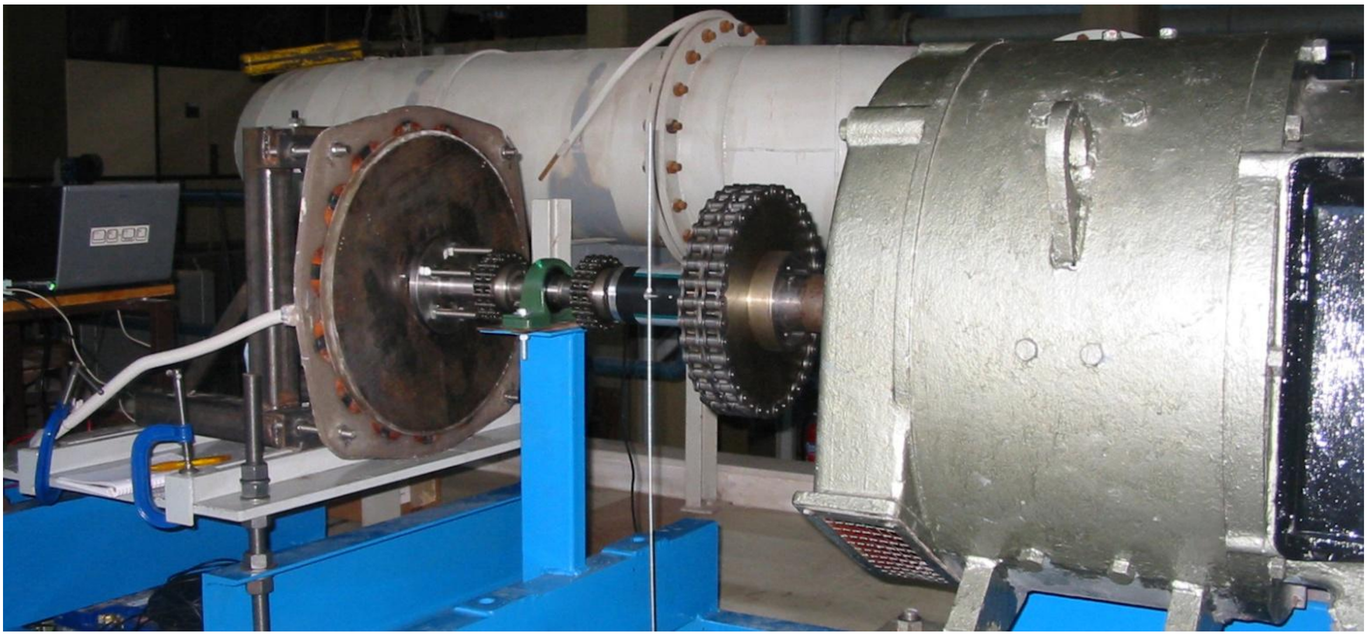

This project has been organized and performed within the framework of the Distributed Energy Resources Research Infrastructures (**DERri**)

in **September 2012** at

The National Technical University of Athens / Institute of Communication and Computer Systems (**ICCS / NTUA**)

by Joerg Alber and Kostas Latoufis

DERri

CAPACITIES

INDEX

1 GENERAL INFORMATION ON THE MEASURING CAMPAIGN

1.1 Introduction

The purpose of this project is to research the performance of locally manufactured **Axial Flux Permanent Magnet (AFPM)** generators, which follow the design explained in Hugh Piggott's building-manual "*A Wind Turbine Recipe Book"* [Piggott].

The main focus of this project is on the applicability of AFPM generators for:

- Small scale wind- and hydro applications, aiming at electricity production.
- Renewable electrification projects.
- Educational purposes within European-wide engineering departments and training centres.

The three different generators subject to this project follow a very simple manufacturing design. It is possible to build them without specialized tools or expertise as well as using basic materials. In fact, the design has been successfully reproduced all over the world, thanks to the mentioned building manual developed by Hugh Piggott[1].

Despite their reproducibility, they are competitive machines, in terms of efficient performance, long term functionality and manufacturing costs. These aspects make them very interesting for a variety of applications, one of them being small scale wind- and hydro-powered systems.

Moreover, the fact this AFPM generator-design can be built in common workshops and by non-professionals, make them a very powerful educational tool. By constructing, testing and analysing such generators, many important concepts of engineering can be applied, making the learning process particularly interesting for educational institutions with a technical focus.

Additional information: Unless specified otherwise, all photos, figures, graphs or tables have been created within this activity or belong to one of the authors. Reproduction must be requested.

[1] http://scoraigwind.co.uk/

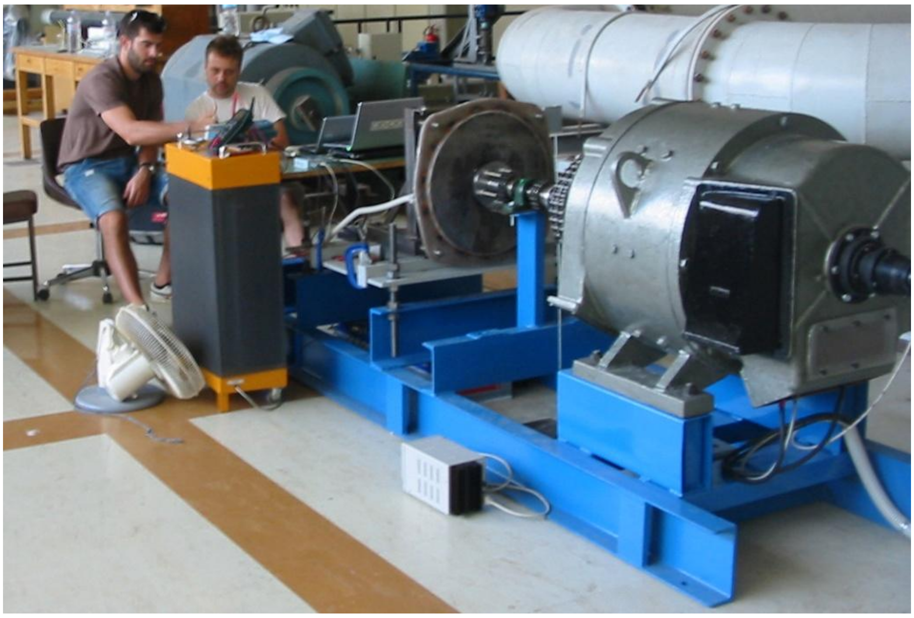

Photo 1: General set-up at ICCS NTUA, Athens

1.2 Basic information

AFPM generators are a branch of 'non-excited' synchronous generators, consisting of three main parts: two rotating steel disks, carrying permanent magnets and one steady stator, carrying the coils of copper wire. The magnets are permanently excited, i.e. they carry a constant magnetic field. The coils are star-connected to a 3-phase system. The rotational movement of the magnet disks induces voltage and current into the stator.

In many synchronous generator designs the magnetic field is created by rotating coils (electro-magnets) which are 'DC-excited' (Fig.4), instead of permanent magnets. The advantages synchronous generators excited by permanent- rather than electro-magnets are:

- No additional power source is required for the excitation of the rotating coils.
- No brushes and slip-rings are needed for the electrical connection of the electro-magnets.

The disadvantages are:

- The magnetic excitation field is constant and cannot be regulated in order to influence the performance of the generator, i.e.to maximise its overall efficiency.
- The mining of raw earths such as Neodym (Nd), which is needed to produce strong enough permanent magnets, entails particularly severe environmental damage and contamination.

The theory of 3-phase electrical systems in star connection will not be explained in detail, as it can be consulted in many publications.

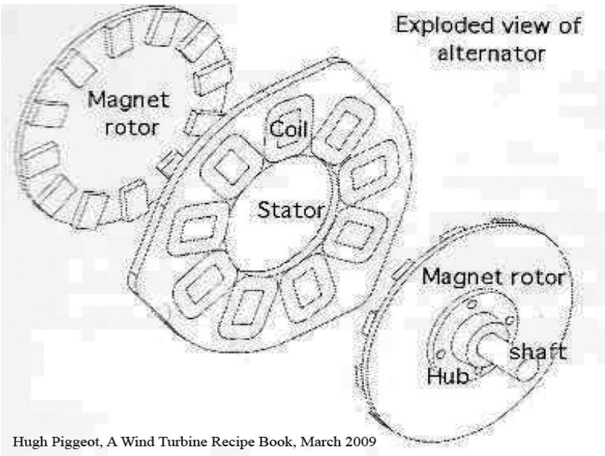

Fig. 1: Main parts of a 3-phase AFPM generator [Piggott]

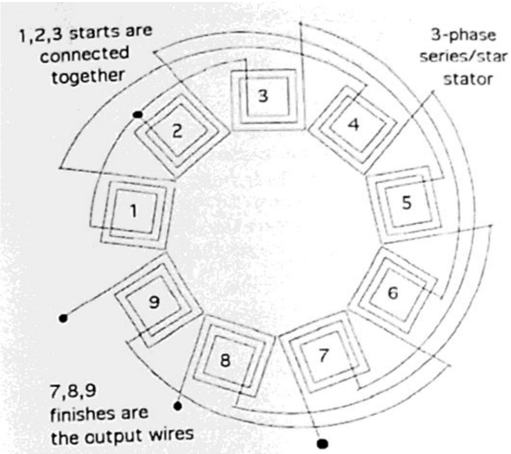

Fig.2: Connection of the copper coils in the stator [Piggott]

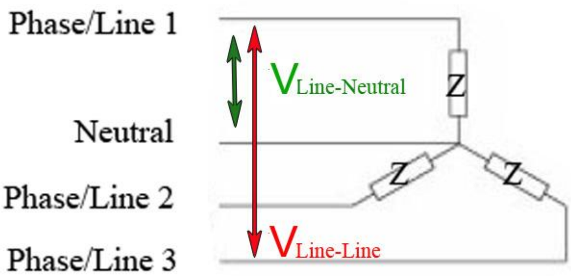

Fig.3: Basic arrangement of a 3-phase star- connection and the different voltages of the system.

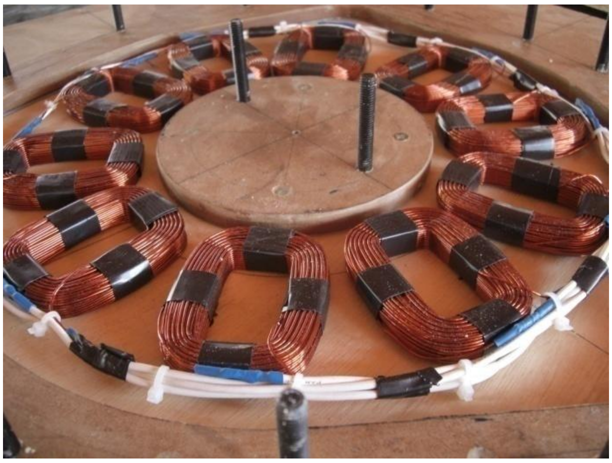

Photo 2: The open stator of an AFPM generator

Photo 3: One magnet disk of an AFPM generator, being casted into polyester resin

Photo 4: The complete generator

Photo 5: The complete wind system

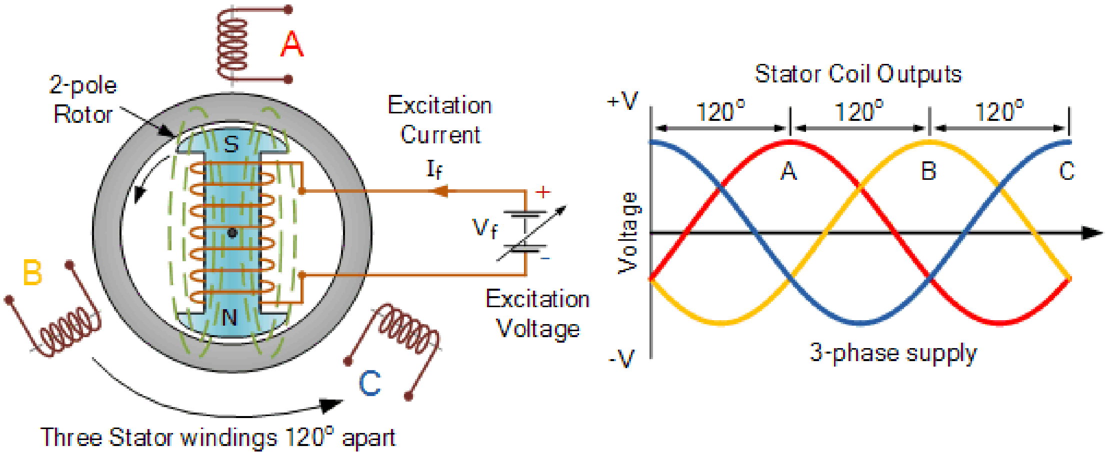

Fig.4: Basic design of a DC-excited synchronous generator producing 3-phase voltage: [*http://www.alternative-energy-tutorials.com*](http://www.alternative-energy-tutorials.com)

AFPM generators need to be designed and constructed in a very precise way in order to do their job properly.

- The magnetic field in between the coils must be as strong as possible: small air gap, strong magnets (high field) and thick iron disks in order to close the magnetic circuits towards the back.

- The heat losses in the coil wires must be minimal: thick wire section, little air between the windings (good quality winding), good heat evacuation on the surface of stator.

- The relation between the magnet-poles (number of magnets) to stator-coils must allow for the required phase difference of φ_{LL}=120° between the three voltage curves, i.e. for 3-phase AC production.

- The magnetic pole-pairs as well as the rotational speed (rpm) of the moving parts must result in exactly the range of voltage needed to either charge a battery system or to feed electricity into the grid: the number of coil-windings must be calculated accordingly.

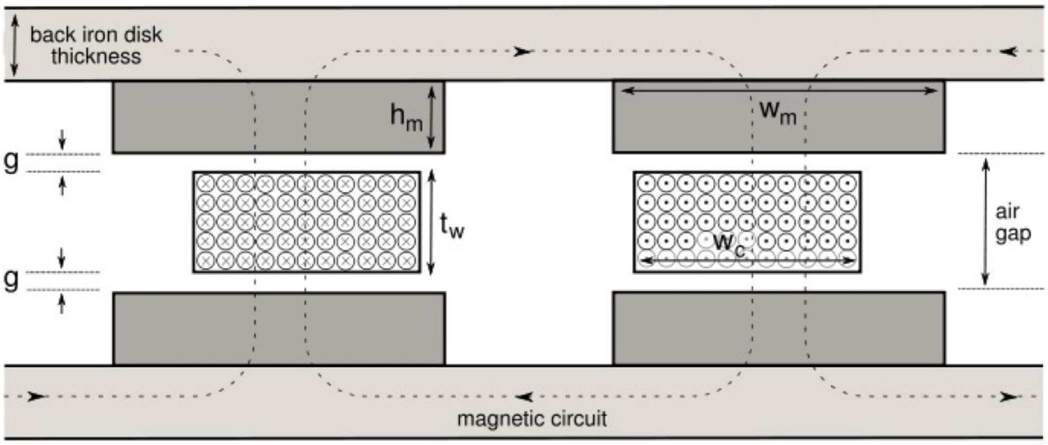

Fig.5: Cross section of an AFPM generator [Latoufis]

8	6	12	9	16	12	20	15	24	18	28	21

Fig.6: Pole to coil relation in 3-phase systems [Latoufis]

The basic equations for voltage, current and power in a **star-connected** 3-phase systems are (Fig.3):

$$V_{LL} = \sqrt{3} \cdot V_{LN} \qquad (1)$$

$$I_{LN} = I_{LL} = I_{AC} \qquad (2)$$

$$S = 3 \cdot \boldsymbol{V_{LN}} \cdot I_{AC} \qquad (3)$$

$$S = \sqrt{3} \cdot \boldsymbol{V_{LL}} \cdot I_{AC} \qquad (4)$$

where
V_{LN} in V corresponds to the line-neutral-voltage,
V_{LL} in V corresponds to the line-line-voltage,
S in VA is apparent power (not including any further conversion losses).

1.3 Subject matter

The measuring campaign consists of detailed performance tests of three different such AFPM generators. The basic generator-data is summarized in the following table.

	'big' generator':	**'medium' generator:**	**'small' generator :**
Rated Power P_{rated}	3000 W	850 W	350 W
Internal connection	3-phase star	3-phase star	3-phase star
Voltage taken	Line-Neutral (L-N)	Line-Line (L-L)	Line-Neutral (L-N)
Rated Voltage V_{rated}	300V (L-N)	85V (L-L)	40V (L-N)
Application	Wind power	Wind power	Hydro power
Connected to	Electricity grid	Batteries, 48 V_{DC}	Electricity grid
Corresponding diameter of rotor blades d	4,34 m	2,4 m	none

Table 1: Basic information on AFPM generators tested

2 TECHNICAL OBJECTIVES OF THE TESTS

- Understanding the performance of the AFPM generators, subject to this measuring campaign (Table 1).
- The scientific analysis of their performance in terms of efficient power production.
- A better understanding of the interaction between such generators and their corresponding rotor blades, so that maximum energy production and life time expectancy can be achieved.
- Setting the foundations for a reliable and efficient measuring campaign in order to reliably check and improve the quality and safety of AFPM generators.
- Setting the foundations for educational courses, particularly laboratory courses on AFPM generators in technical universities and institutes.
- Finally, contributing to the development of Open Source Hardware[2] in the renewable energy sector.

3 TESTS EXECUTED

Different test have been executed with the generators described in Table 1:

Test No.	Small generator	Medium generator	Big generator
1	Open Circuit Voltage	Open Circuit Voltage	Open Circuit Voltage
2	Torque vs Current	Torque vs Current	Torque vs Current
3	Internal resistance	Internal resistance	Internal resistance
4	---	---	AC/DC rectification under additional load
5	---	Battery connection	---
6	---	Battery connection and additional load	---
7	---	Interaction between generator and rotor blades under battery connection	---

Table 2: Summary of executed Tests

[2] http://en.wikipedia.org/wiki/Open-source_hardware

4 RESULTS

At the beginning of each Test, the general set-up, purpose, measuring instruments and a summary of results is being specified. This structure allows for a general overview before reading through each specific and detailed test procedure.

In addition, the following points are relevant for the understanding of this report:

- It is important to note, that the given measuring instruments for **rpm and torque** are inaccurate. This has two important consequences:

  1.) In general, it is the very precise electrical frequency, which is used as the reference for rpm.

  2.) All results which depend on the torque are not precise.

- In the sections 'Results in detail' of each Test, **exemplary graphs and figures** are analysed**,** which represent the specific measuring campaign.

- The tests are organized **chronologically**, i.e. further test are based on the explanations and results that earlier test have provided.

- All AC-values of this report are expressed as **rms (root mean square)- values**, which is the most common way of expressing AC signals as their effective DC equivalence. Whenever relevant, the index of the electrical values in question are specified, e.g. as line-neutral V_{LN} or line-line V_{LL} voltage.

4.1 Test 1: Open Circuit Voltage (all generators)

Set-up:

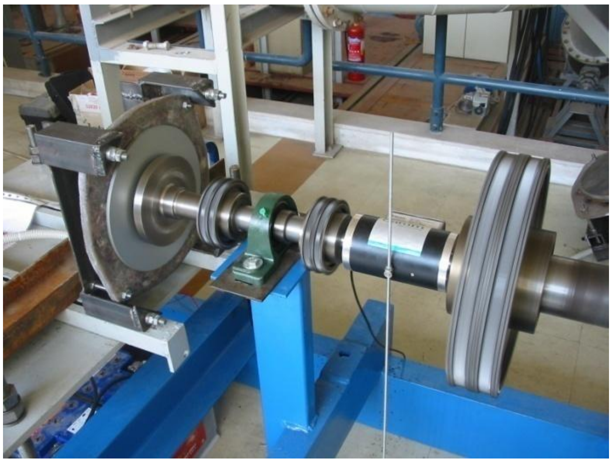

Photo 6: Test 1

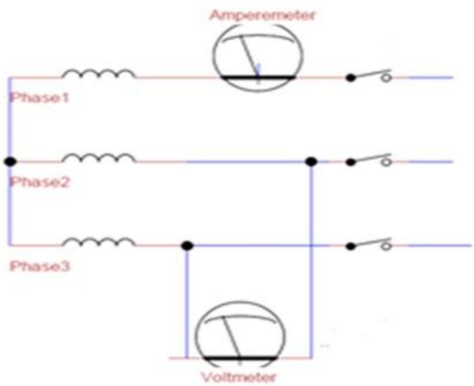

Fig.7: Set-up of Test 1

The generator is on open circuit (OC), thus no current can be flowing. The rpm are modified within the specific range of the generator (see below).

Purpose: Analysing and comparing the performance of all generators at different rpm and no current-flow, in terms of voltage per rpm, pole-pair number, phase difference and harmonics.

Instruments: Oscilloscope and torque meter.

Summary of results:

- The rpm-range of each generator depends on the rotor diameter: the bigger the respective rotor diameter, the lower the rpm-range.
- The rpm increase proportionally to the open circuit voltage: An analogy between mechanical rpm and electrical open circuit voltage can be shown.
- The relation between open circuit voltage and rpm can be expressed through a proportionality-factor.
- The constant relation between electrical frequency and mechanical rpm is set by the pole-pair number of the generator.
- The phase difference between the sinusoidal voltage-curves of a three phase system is $\varphi_{LL} = 120°$.
- The curves of the open circuit voltage are very 'clean', hardly any harmonics can be detected.

Results in detail:

1.) Since the open circuit voltage is measured in relation to rpm, the operational rpm-range of each machine must be defined. The generators are designed to be driven by rotor blades, which turn wind energy into rotational power. The rotor blades' performance in the wind is defined by their designed tip speed ratio:

$$TSR = \frac{u}{v} = \frac{\pi \cdot d \cdot rpm}{60 \cdot v} \qquad (5)$$

where
TSR is the dimensionless tip speed ratio,
u is the rotational speed of the tip of the blade in $\frac{\mathrm{m}}{\mathrm{s}}$,
v is the wind speed in $\frac{\mathrm{m}}{\mathrm{s}}$,
rpm is revolutions per minute in $\frac{1}{min}$,
d is the rotor diameter in m.

According to (5), the rpm-range of each set of rotor blades can be calculated as follows:

$$rpm = \frac{60 \cdot TSR \cdot v}{\pi \cdot d} \qquad (6)$$

Wind speeds between $3\frac{m}{s} < v < 10\frac{m}{s}$ are considered realistic values for small-scale systems. For $v > 10\frac{m}{s}$, a mechanical braking mechanism kicks in to protect the rotor from damage due to excessive centrifugal forces.

According to Hugh Piggott, the blades of all generators are designed for TSR ≈ 7. In accordance with most state-of-the-art wind turbine designs, the rotational speed of the blade-tip is supposed to be 7 times higher than the attacking wind speed. The blade-diameter is chosen according to Table 1.

big	**medium**	**small**	
100 < rpm < 300	170 < rpm < 550	220 < rpm < 750	rpm-range in $\frac{1}{\min}$

Table 3: rpm-range of all generators

The bigger the blade diameter, the lower the rpm-range.

2.) The open circuit voltage increases linear with rpm. Since there is no current, no torque can be detected.

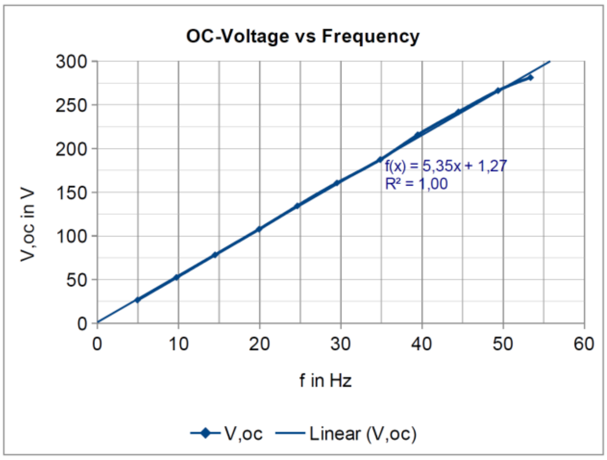

Graph 1: Open circuit measurement, big generator

The different values make a linear relation. The electrical open circuit voltage and the mechanical rpm are directly related to each other.

3.) The proportional relation of 2.) can be expressed as one average and constant proportionality-factor of the form:

$$\frac{V_{OC}}{rpm} \qquad (7)$$

small	**medium**	**big**	**comments**
$0{,}0502\,\frac{\mathrm{V}}{\min}$	$\left(\frac{0{,}165}{\sqrt{3}}\right) = 0{,}095\,\frac{\mathrm{V}}{\min}$	$0{,}9\,\frac{\mathrm{V}}{\min}$	In accordance with equation (1), all results are expressed as line-neutral values.

Table 4: Average constant voltage per rpm- factor

4.) The frequency of the generator depends on its pole- pair number: Taking the medium generator as an example, each rotor disk consists of 12 magnets, i.e. 6 North- and 6 South- poles facing the coils. Every **pole** (magnet) creates half a sinusoidal cycle of φ=180° or half a sinusoidal period, each **pole pair** a full sinusoidal cycle of φ=360° or one full sinusoidal period when passing over one coil or phase (Fig.4). The number of magnetic poles is therefore double the amount of the pole-pair number.

Hence, the change in magnetic polarity, North to South (N-S), is reflected by the change in electrical polarity from positive to negative. For instance, the 12 magnets of the **medium** generator provoke six full sinusoidal cycles in each set of coils (or phase) per 1rpm. The fact that the stator is sandwiched by two rotor disks increases the magnetic flux, thus voltage output.

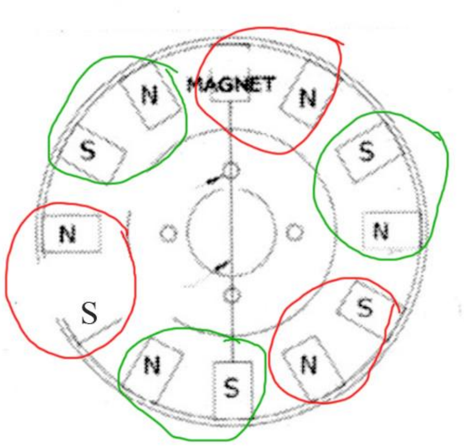

Fig.8: Top view of one magnet disk with each pole-pair marked, medium generator [Piggott, modified]

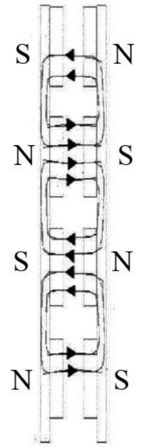

Fig.9: Rotor disk- sandwich with magnetic field lines between the magnets and through the steel disk [Piggott, modified]

The pole pair number determines the constant relation between rpm in $\frac{1}{\mathrm{min}}$ and frequency f in $\frac{1}{\mathrm{s}}$:

$$p = \frac{60 \cdot \mathrm{f}}{\mathrm{rpm}} \qquad (8)$$

where

f is frequency in $\frac{1}{s}$ or Hz,

and p the pole-pair number.

Depending on each generator design, a constant factor k can be defined as to easily convert rpm into frequency and vice versa:

$$f = \frac{\mathrm{rpm}}{\mathrm{k}} \qquad \text{or} \qquad rpm = \mathrm{k} \cdot \mathrm{f} \qquad (9)$$

small	medium	big	
4	6	10	Pole pair- number or full sinusoidal cycles per phase and rpm.
15	10	6	Constant factor k

Table 5: Pole pair numbers and direct proportionality between rpm and frequency

5.) The phase difference between each voltage-phase can be shown on the oscilloscope:

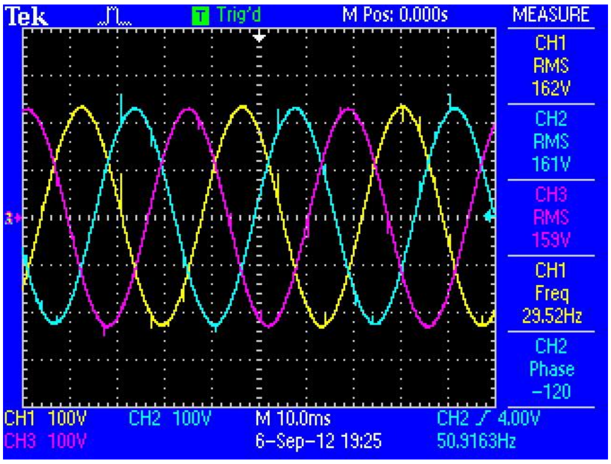

Fig.10: OC-measurements line-neutral at normal operation (30 Hz=180 rpm), big generator

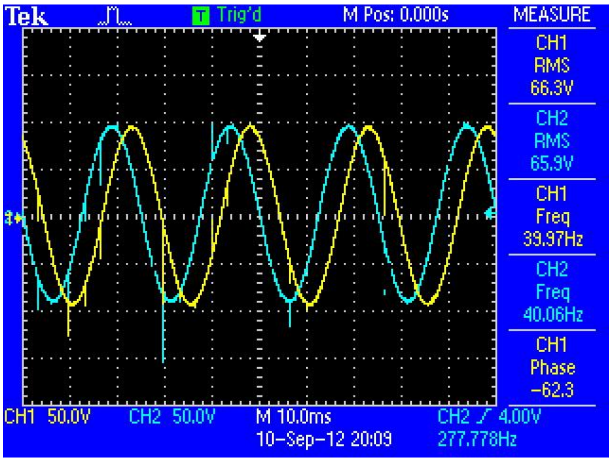

Fig.11: OC-measurements line-line at normal operation (40 Hz=400 rpm), medium generator

When executing line-line measurements, one of the three lines has to act as the corresponding or reference line. Hence only two AC curves can be seen when measuring line-line in Fig.11.

small	**medium**	**big**	
120°	60°	120°	Phase difference φ_{LL}

Table 6: Phase differences between voltage curves

For 3-phase machines is $\varphi_{LL} \approx 120°$, as shown in Fig.10. In case of the medium generator (Fig.11) $\varphi_{LL} \approx 60°$, which suggests either a systemmatic measuring error or constructive mistakes regarding the alignment of the coils in the stator. The very reason for this phenomena could not be answered conclusively. As shown furtheron in Tests 2 and 5, the performance and efficiency of the medium generator does not suffer in comparison with the other generators tested. The mentioned results are therefore considered to be caused by a systematic measuring error.

6.) The analysis of harmonics, based on the fourier series, reveals how ‘clean' the overall AC signal is. Harmonics are an integer multiple of the fundamental or dominant rotational frequency. Once the signal is distorted by harmonics, the main frequency becomes a mix of many different sinusoidal signals at once. The less harmonics, the better or cleaner the signal.

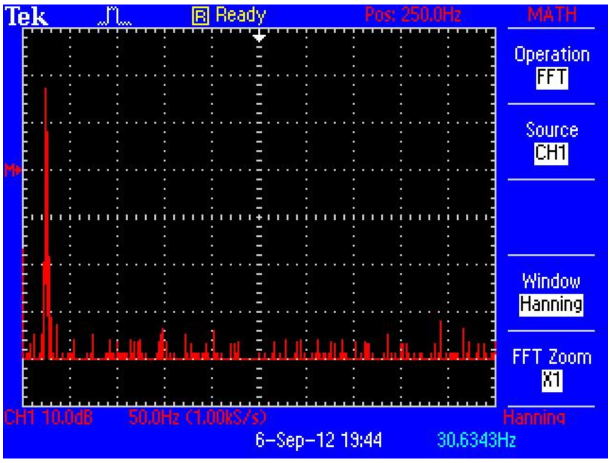

Fig.12: Fourier-series at 30 Hz = 180 rpm, big generator

The voltage signal of phase 1 (CH1) in Fig.12 consists mainly of the predominant rotational frequency of 30,6 Hz. Hardly any harmonics, other than normal background noise, can be detected. A clean signal suggests little losses due to distortion within the electrical system and little mechanical vibrations and noise during operation. In fact, in an open circuit situation there are no losses, since no power is generated.

4.2 Test 2: Torque vs current (all generators)

Set-up:

Photo 7: Test 2

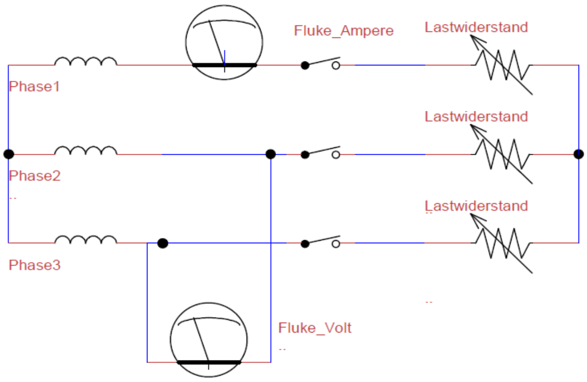

Fig.13: Set-up of Test 2

The generator is connected to a variable 3-phase ohmic load **at constant rpm**. The amount of current can be changed by modifying the resistance, according to

$$I_{rms} = \frac{V_{rms}}{Z} \qquad (10)$$

where

Z is the impedance (complex resistance) in Ω,

I_{rms} is the AC-current in A,

V_{rms} is AC-voltage in V.

Note: For an ohmic load is Z = R.

Test 2 is the only experiment under (ohmic) load, which can be executed with all three generators, making them directly comparable between each other.

Purpose: Analysing **and comparing** the performance of the generators in relation to varying current intensity, in terms of mechanical torque, mechanical/electrical power, voltage, harmonics and efficiency.

Instruments: Oscilloscope and torque meter.

Summary of results

- The torque increases proportionally to the current: An analogy between mechanical torque and electrical current can be shown.
- Voltage and current act proportionally to each other at constant rpm: the higher the current, the lower the voltage and vice versa.
- The harmonics increase under load, as electrical power is generated.
- Efficiency is the dimensionless relation between the electrical power output and the mechanical power input. It makes the performance of all electrical generators comparable with each other, independently of their sizes. It is one of the most important quality aspects.
- The efficiency of each generator correlates with the amount of harmonics they produce: the more harmonics, the lesser the efficiency.
- Both big and medium generator show good efficiencies, similar to commercial products. The small generator turns out to be subject to poor efficiencies.

Results in detail:

1.) The mechanical torque increases proportionally to the current at constant rpm.

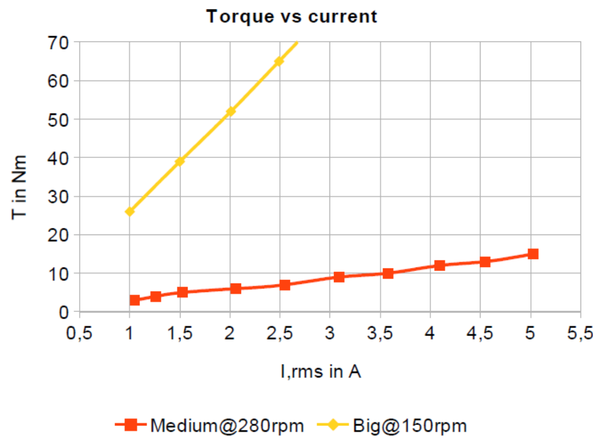

*Graph 2: Linear relation between torque and current at **moderate** rpm, big and medium generator*

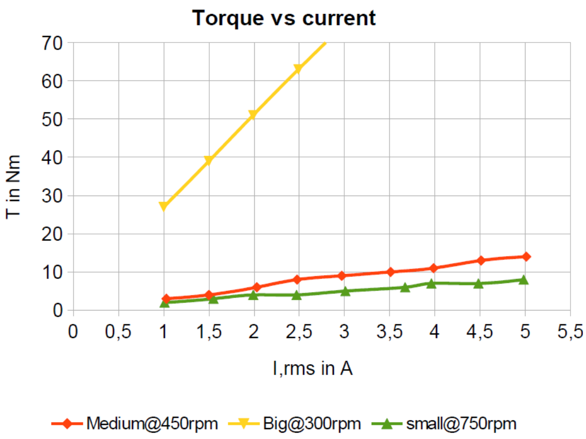

*Graph 3: Linear relation between torque and current at **rated** rpm, all generators*

The small generator has only been tested for rated rpm, hence does not appear in Graph 2. These linear relationships show the analogy between the mechanical torque and the electrical current.

2.) The mechanical power, on the other hand, is dependent on both, torque and rpm:

$$P_M = 2 \cdot \pi \cdot T \cdot \frac{rpm}{60} \qquad (11)$$

where

P_M is mechanical power in W,

T is torque in Nm,

rpm is revolutions per minute in $\frac{1}{\text{min}}$.

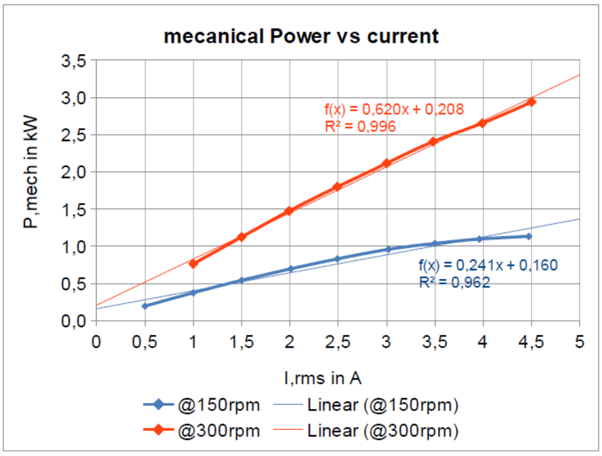

Graph 4 : Relation between current and mechanical power at constant rpm, big generator

The maximum power output is limited by heat losses in the wires (see blue curve in Graph 4 at high currents). In this test, the maximum surface temperature of the stator has been measured at $t \approx 80°C$. Above, additional ventilation (here wind) must be provided to avoid the fibre glass resin and wires from getting damaged.

3.) The linear voltage/current dependency which is typical for all electrical energy sources can be shown: The higher the current, the lower the voltage and vice versa (due to the internal resistance of the power source).

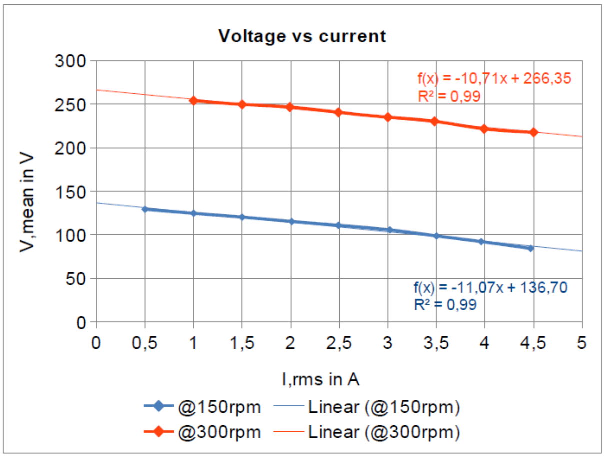

Graph 5: Relation between voltage and current, big generator

4.) The wave forms, i.e. harmonics are visibly more ‘noisy’ than in Test 1: The generators are now actually generating power.

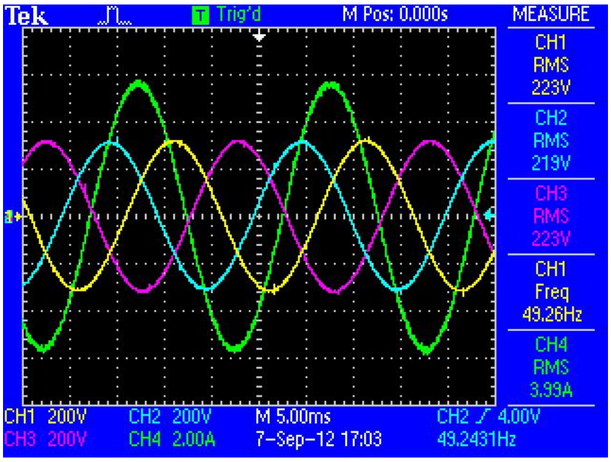

Fig.14: Wave form at rated rpm and high currents (green), big generator

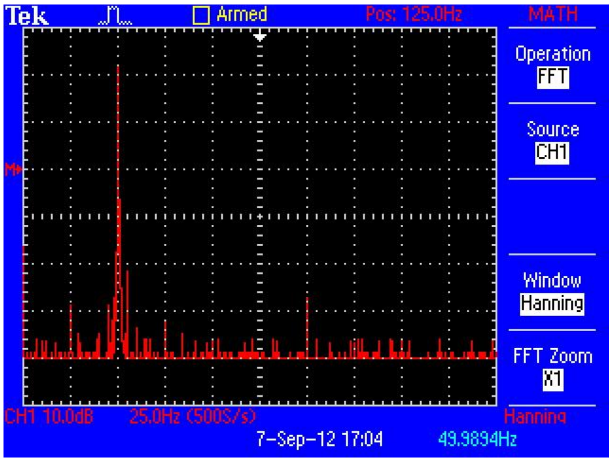

Fig.15: Fourier series at rated rpm and high currents, big generator

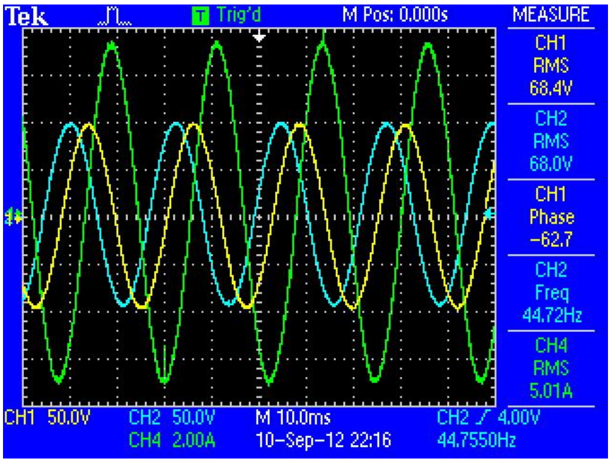

Fig.16: Wave form at rated rpm and high currents (green), medium generator

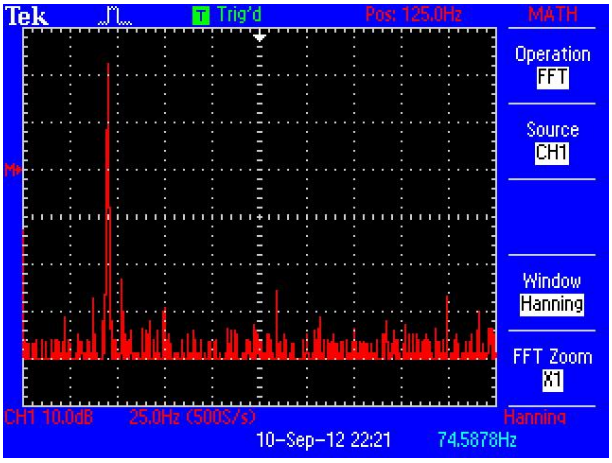

Fig.17: Fourier series at rated rpm and high currents, medium generator

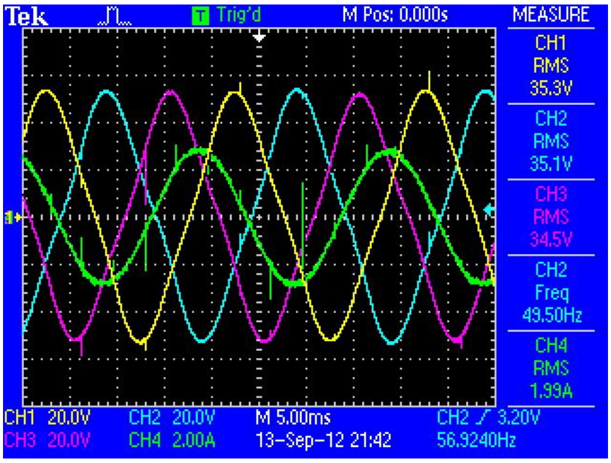

Fig.18: Wave form at rated rpm and moderate currents (green), small generator

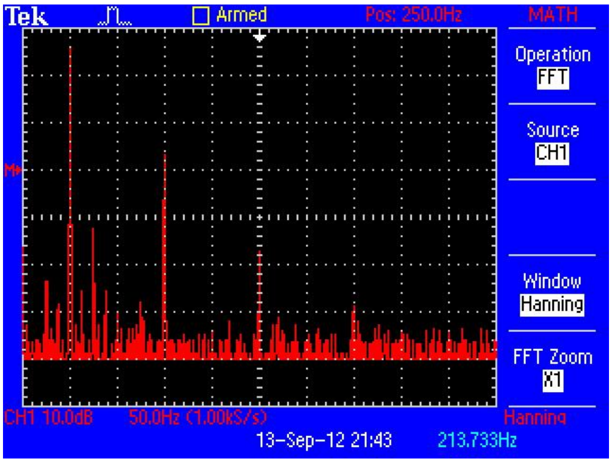

Fig.19: Fourier series at rated rpm and moderate currents, small generator

The level of harmonics is one important reason for losses, since parts of the generated electrical power gets lost in the system. In fact, some of the different frequencies can be detected as 'noise', i.e. vibration and/or buzzing of the generator. These kinds of losses reflect back on the overall efficiency, since less mechanical power is turned into electrical power. Otherwise it is very difficult to clearly quantify them.

Comparing Fig 14-19 above, the big generator has least harmonics, followed by the medium one, which shows them quite clearly, and finally the small generator, which gives the worst results.

5.) The efficiency is the dimensionless relation between the electrical power output and the mechanical power input. It makes the performance of all electrical generators comparable with each other, independently of their sizes. It is one of the most important quality aspects.

$$\eta = \frac{P_{out}}{P_{in}} = \frac{P_{electrical}}{P_{mechanical}} < 1 \qquad (12)$$

The AC-efficiency, as the relation between apparent power and mechanical power is defined as

$$\eta_{AC} = \frac{S}{P_M} \qquad (13)$$

where
S is apparent power in VA (not including any further conversion losses),
$P_M = P_{Mech}$ is mechanical power in W.

The DC-efficiency, as the relation between effective or direct power and mechanical power is defined as

$$\eta_{DC} = \frac{P_{DC}}{P_M} \qquad (14)$$

where
P_{DC} is direct power in W,

In terms of efficiency results, two phenomena are to be expected:

a) Higher currents → more heat losses → less electrical power output in relation to mechanical power input → poorer efficiency.
.
b) Higher constant rpm → higher voltage → similar losses → more electrical power output in relation to mechanical power input → better efficiency.

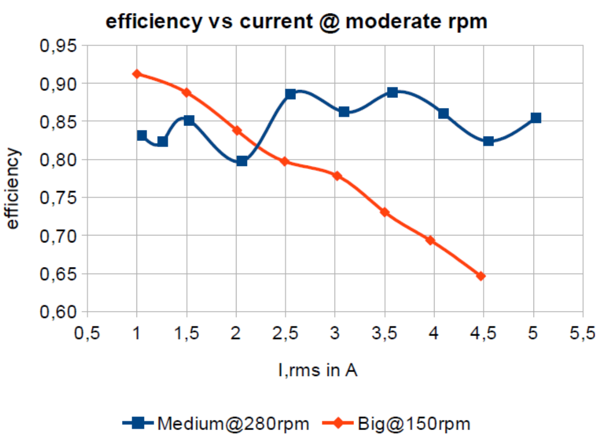

*Graph 6: Efficiency of apparent power at **moderate** rpm, medium and big generator*

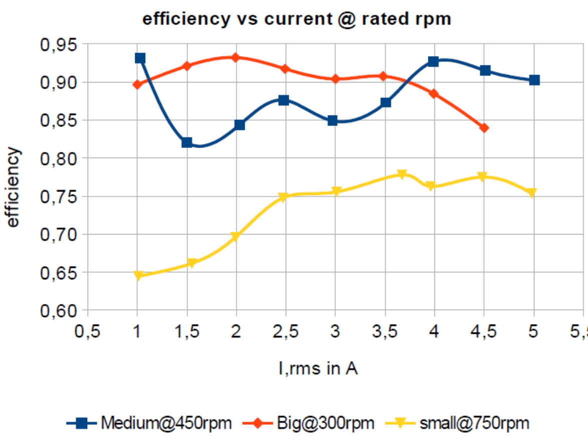

*Graph 7: Efficiency of apparent power at **rated** rpm, all generators*

The small generator has only been tested for rated rpm, hence does not appear in Graph 6.

Graphs 6 and 7 show the relation between electrical power output versus mechanical power input. Due to the mentioned and inaccurate indication of the torque meter (explained in chapter 3) none of the two graphs can be considered very precise.

However, three common phenomena regarding the efficiency of AFPM generators can be extracted from the above graphs:

a) At start- up ($0\ \mathrm{A} < \mathrm{I_{AC}} < 2{,}5\ \mathrm{A}$): Increasing current → higher magnetic field around the coils → more magnetic friction between permanent magnets and coils, i.e. torque → higher power output → higher efficiency.

b) At normal and rated performance ($I_{AC} > 2{,}5\ A$): High current → more heat losses → less electrical power output in relation to mechanical power input → poorer efficiency.

.

c) Increasing rpm → higher voltage → similar losses → more electrical power output in relation to mechanical power input → better efficiency.

The mentioned phenomena do partly counteract and contradict each other and are very difficult to understand as a complete system. In terms of the testing results, the big generator shows the best efficiencies with $\eta_S \approx 90\%$, followed by the medium one with $\eta_S \approx 85\%$ The small machine falls behind with $\eta_S < 80\%$. Looking at the fourier distribution of the previous point, a correlation between the amount of harmonics and the efficiency-levels can be appreciated: the apparent power S decreases as harmonics increase.

The following datasheets show AC-efficiencies of similar commercial AFPM generators with different operating points (much higher rpm), but a similar rated power output, given as apparent power in kVA.

Type series 080 Rated Power: 0.5 - 1.5 kVA / Depending on rpm

PGS 080
Weight ca. 3.9 kg

Generator Speed [min⁻¹]	Rated Power [kVA]	No load voltage (% of rated Voltage)	Short circuit current (% of rated current)	Efficiency
1500	0.55	115	325	83 %
3000	1.0	114	338	85 %
4500	1.3	113	360	87 %
6000	1.5	112	400	88 %

Type series 100 Rated Power: 1.1 - 3.0 kVA / Depending on rpm

PGS 100
Weight ca. 6.8 kg

Generator Speed [min⁻¹]	Rated Power [kVA]	No load voltage (% of rated Voltage)	Short circuit current (% of rated current)	Efficiency
1500	1.1	115	330	84 %
3000	2.0	114	330	90 %
4500	2.5	113	335	91 %
6000	3.0	112	370	91 %

Fig.20: Datasheet[3] of synchronous permanent magnet generators, http://www.heinzmann.com

Both the medium and big generator are perfectly able to compete with the data given in Fig.20.

6.) Addition: The anomaly of the phase-difference-measurement of φ_{LL} = 60° between the open-circuit-curves of the medium generator (Test 1) does not have any obviously negative impact on its specific efficiency. Consequently the reason for this unexpected and unrealistic phase angle is most probably a systematic measuring error, which in case of the medium generator had to be taken between two phases rather than phase and neutral line.

4.3 Test 3: Stator resistance (all generators)

Set-up / Purpose: Measuring the internal ohmic stator resistance between each phase at working temperature.

Instruments: DC- supply.

Summary of results

- The stator resistance depends on the number of turns and the cross section of the wire used.
- The stator resistance depends on the voltage output required: high voltage requires many turns, thus thin wire.
- The heat-losses in the wire can be calculated for each phase with

$$P_{\text{heat,Phase}} = R_{\text{i,Phase}} \cdot I_{AC}^2. \qquad (15)$$

where

$P_{\text{heat,Phase}}$ is power as heat-loss per phase in W,
$R_{\text{i,Phase}}$ is the internal resistance per phase in Ω.

Results in detail:

	big	**medium**	**small**
Coil-windings per coil	337	90	146
Number of coils per phase	5	3	2
Cross section of wire in mm^2	0.71	1.77	1.37
Average internal ohmic resistance per phase	8.97 Ω	0.61 Ω	1.01 Ω
e.g.: heat-loss in the stator for $I_{AC} \approx 1$ A in W	27 W	accordingly	accordingly
e.g.: Heat-loss in the stator for $I_{AC} \approx 3$ A in W	242 W	accordingly	accordingly
e.g.: Heat-loss in the stator for $I_{AC} \approx 5$ A in W	672 W	accordingly	accordingly

Table 7: Stator resistance per phase of each generator

[3] http://www.heinzmann.com/de/motor-und-turbinen-management/download-etm/doc_download/1633-overview-synchronous-generators

The current-flow of each generator depends on its output voltage: the higher the designed voltage output, the lower the total current flow, thus generation of heat.

The very importance of heat evacuation, in this case provided by the wind, is emphasized by the exemplary heat loss calculation for the big generator in Table 7.

4.4 Test 4: AC/DC-rectification under ohmic load (big generator)

Set-up:

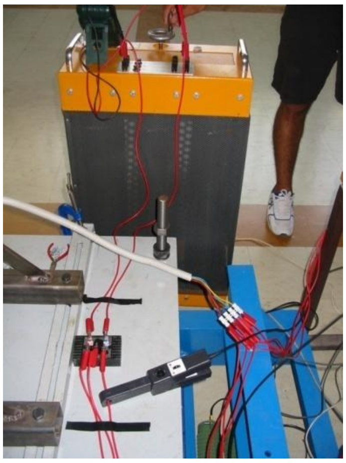

Photo 8 : Test 4, bridge rectifier (black box on the table)

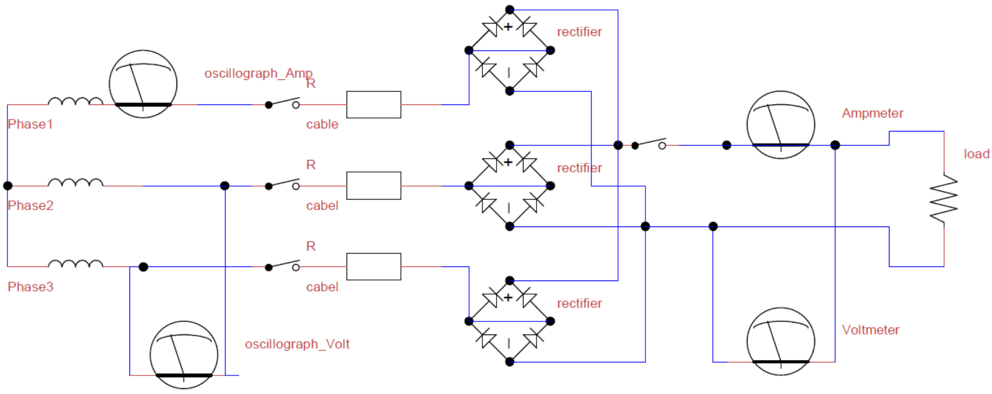

Fig.21: Set-up for Test 4

Only the **big generator** is connected to a bridge rectifier, feeding a variable ohmic load of R = 106,8 Ω, being able to dissipate a maximum current of I_{max} = 5A.

Purpose: Analysing the performance of the big generator connected to a DC-bridge-rectifier plus an additional ohmic load at different rpm, in terms of harmonics, efficiency and the AC/DC-voltage-ratio.

Instruments: Oscilloscope, torque meter and multimeter.

Summary of results:

- The harmonics increase visibly when connecting the generator to an AC/DC bridge rectifier, resulting in significant additional losses.
- Comparing AC- and DC-efficiency, the losses in the rectifier can be shown.
- The mean ratio between DC- and 3-phase-AC-voltage confirms the conversion number 2.34, usually given in respective publications for bridge rectifiers.

Results in detail:

1.) Connecting the generator to a bridge-rectifier has a distorting effect on the wave form, i.e. the harmonics increase drastically.

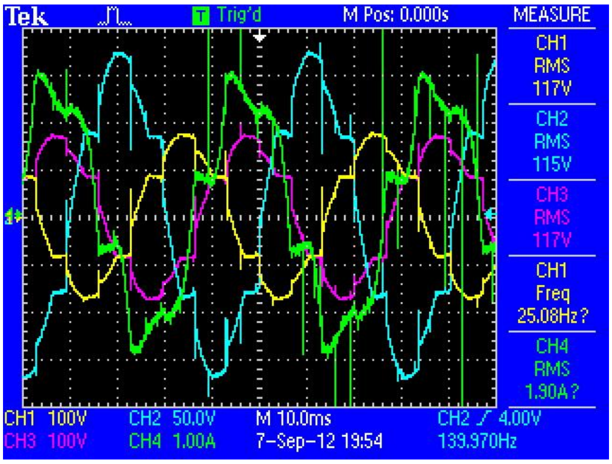

Fig.22: Voltage and current waveforms under rectification at rpm=150rpm, big generator

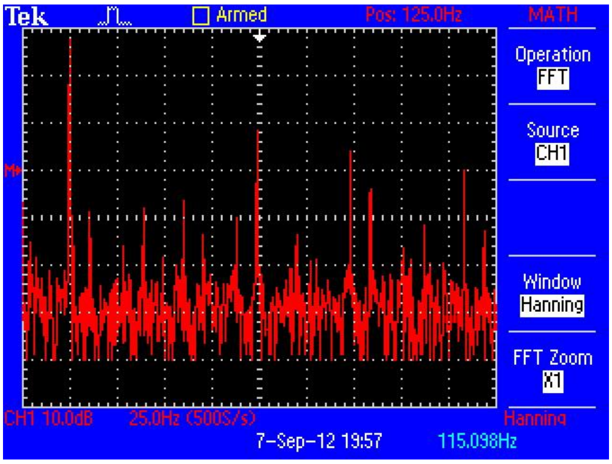

Fig.23: Frequency distribution under rectification at rpm=150 rpm, big generator

According to the fourier series, the AC-signal is now a mix of many different sinusoidal waves. This is a normal symptom when turning (forcing) AC into DC. The more distorted the sinusoidal signals, the more losses occur in the process.

2.) The losses of the rectification process become visible, when comparing AC- and DC- efficiency:

$$\Delta\eta = \eta_{AC} - \eta_{DC} \qquad (16)$$

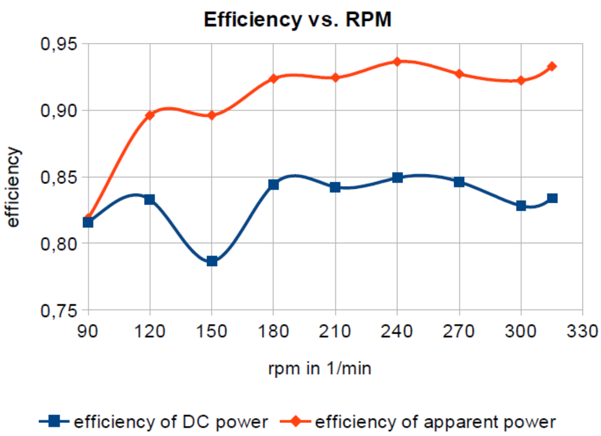

Graph 8: Efficiencies, big generator

The difference between both curves goes back to the overall power drop, i.e. losses in the bridge-rectifiers, which accounts for as much as $\Delta\eta \approx 7\%$. The AC-efficiency itself, i.e. the generation of apparent power, is similar to the results of Test 2 (without rectification).

3.) The mean ratio between AC- and DC-voltage is: $\frac{V_{DC}}{V_{AC}} \approx$ *2.17*. This is relatively close to the value of 2.34, generally given in respective publications for 3-phase AC to DC conversion by means of bridge rectifiers.

4.5 Test 5: Battery connection (medium generator)

Set-up:

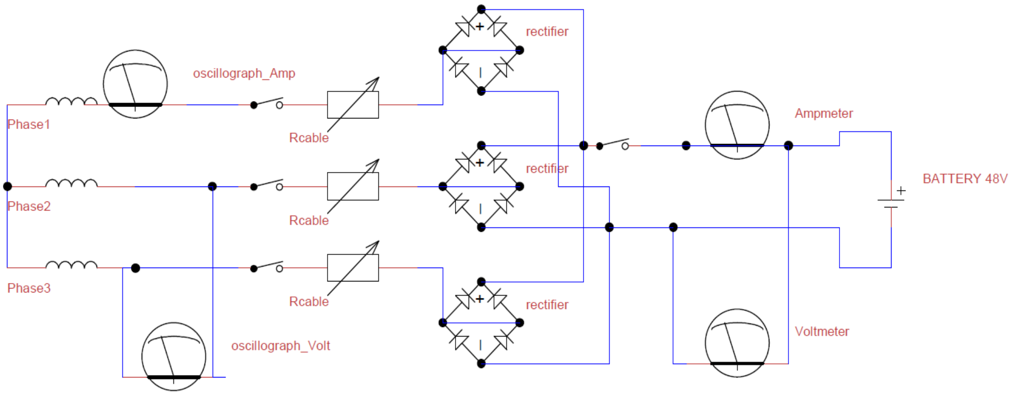

Photo 9: Test 5, Battery connection

Fig.24: Set-up for Test 5

Only the medium generator is connected to a battery bank of 4 typical deep-cycle lead-acid batteries via the bridge-rectifier of the previous Test. The battery-arrangement determines the AC/DC-voltage-range of the whole system, by keeping (forcing) the DC-voltage into the required voltage-range of $46V < V_{Batt} < 58V$. Voltage levels outside this interval damage or even destroy them. An adequate charge controller must impede the batteries from voltage levels outside this interval.

Purpose: Analysing the performance of the medium generator under battery connection at different rpm and different cable resistances between generator and batteries, in terms of its AC/DC performance, power output, harmonics and efficiencies.

Instruments: DC- supply, oscilloscope, torque meter and multimeter.

Summary of results:

- The cable resistance between generator and batteries has a significant impact on the generator's current-flow, thus torque and power generation: too much torque on the generator provokes the rotor blades to stall, i.e. not being able to extract the kinetic energy from the wind efficiently. Too little torque on the other hand makes the rotor spin very fast, but with hardly any power being generated.

- The harmonics increase visibly for a battery connection via bridge rectifier, resulting in high distortion losses.

- The overall efficiency between the driving force down to the batteries is expressed by the DC-efficiency, which is significantly lower compared to the AC-efficiency of previous Test 2.

- Low cable resistances, i.e. short cables give good results for low rpm or wind speeds, while in the range of high rpm or wind speeds the efficiency suffers significantly. It is important to define the most appropriate constant cable resistance (length) depending on the wind situation of a given location as well as the assumed voltage level of the batteries.

Results in detail:

1.) The different possible cable resistances between generator and rectifier are measured using a DC-supply:

	3 x 1m cable	**3 x 20m cable**	**3 x power resistor**
Resistance R_{cable}	0.01 Ω	0.18 Ω	4.83 Ω
Area cross section A_{cable}	2.5 mm^2	2.5 mm^2	Photo 10

Table 8: Different cable resistances applied

The resistances used according to Table 8 are arbitrary. Since high currents are applied, the resistors must be especially strong, while not heating up to much, as heat falsifies the results. Since no variable ohmic power load of this size is available, three ceramic power resistors have been connected in series with the generator cables, simulating a very long cable of almost 700 meters at $\mathrm{A_{cable}} = 2{,}5\ \mathrm{mm}^2$.

Photo 10: Power resistors connected in series
to simulate a large cable length of approximately 700 meters

2.) For further measurements, the relevant rpm-range of the **medium** generator is defined according to Table 3: $170 \frac{1}{min} < n < 550 \frac{1}{min}$.

Higher rpm result in proportionally higher open circuit voltage. Since the batteries determine or ‘force’ the generator’s voltage into the required range, higher rpm necessarily translates into higher currents. The system voltage on the other hand only increases slowly as the batteries recharge.

At the same time a higher constant cable resistance results in less current flow, thus less torque on the generator (Test 2). If our system was a bike, a very long or thin cable would resemble a low gear (high rpm/low torque) and vice versa.

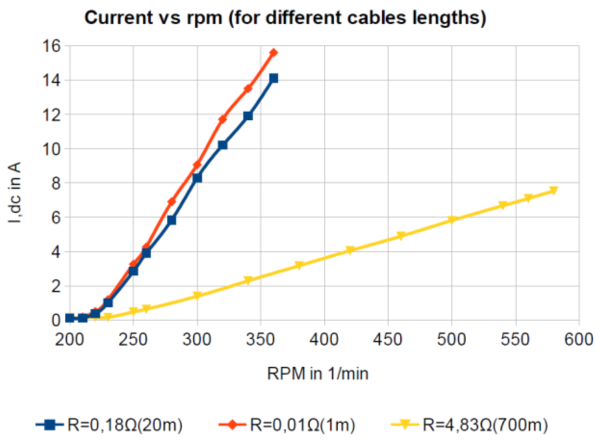

Graph 9: Current vs. rpm for different cable resistances, medium generator

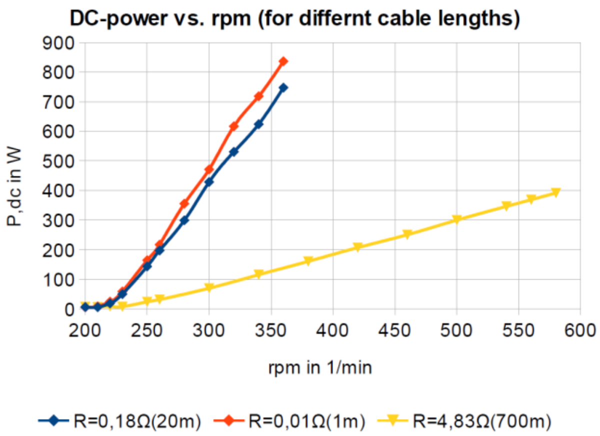

Graph 10: DC-power vs. rpm for different cable resistances, medium generator

Graph 9 and 10 show that the cable resistance is a crucial factor when matching generator and rotor blade performance in order to gain maximum power output thus efficiency: high torque (i.e. high current) on the generator provokes the rotor blades to stall, i.e. not being able to extract the kinetic energy from the wind efficiently. Low torque (i.e. low current) on the other hand makes the rotor spin fast, but with little power generation.

In fact, applying R_{cable} = 4.83 Ω (yellow curve above), current and power increase only very smoothly with rpm, resulting in very poor overall power output. Applying R_{cable}=0.01 Ω, the increase is very steep, resulting in poor power output at higher wind speeds, since the rotor blades tend to stall at relatively low rpm (see Test 7 below).

3.) For battery-connected systems, increasing current makes the battery-voltage to rise proportionally, i.e. makes the batteries to recharge faster.

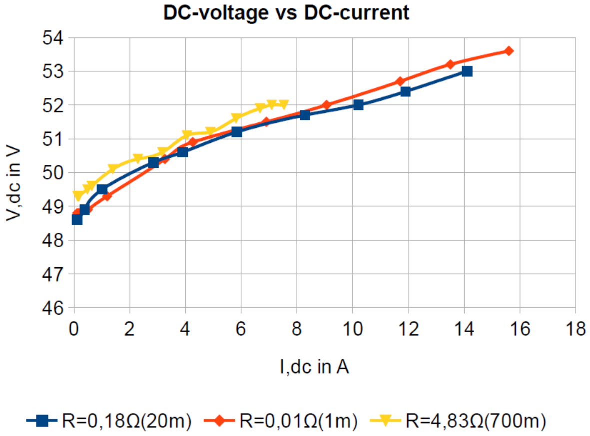

Graph 11: Batteries gaining voltage with current (recharging) for different cables resistances, medium generator

Graph 11 shows that the system is far off $V_{Batt,max}$ = 58V. In fact, for $I_{batt} \approx 0A$, the state of charge of the batteries at open circuit can be appreciated. In all three cases it is at the lower limit of the acceptable charge-voltage.

It should be noted, that the recharging process of a battery bank is a rather slow process. Applying a high current-flow, the battery, i.e. DC-voltage rises immediately. Equally, reducing the current-flow after a short amount of time again (less than 30 min), the open circuit battery voltage will not have increased significantly, i.e. the battery will have only filled up a little bit.

4.) As expected from the results of Test 4, the wave form distortion under battery connection is rough. The fourier series reveals a complicated mixture of frequencies in the signal. The following graphs look similar, independently from the cable resistance applied.

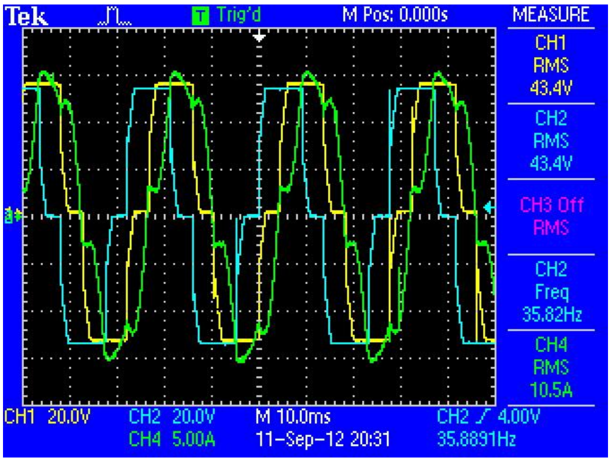

Fig.25: Voltage of Phase 1 and 2 (green, yellow) and current (blue) @ 360 rpm, medium generator

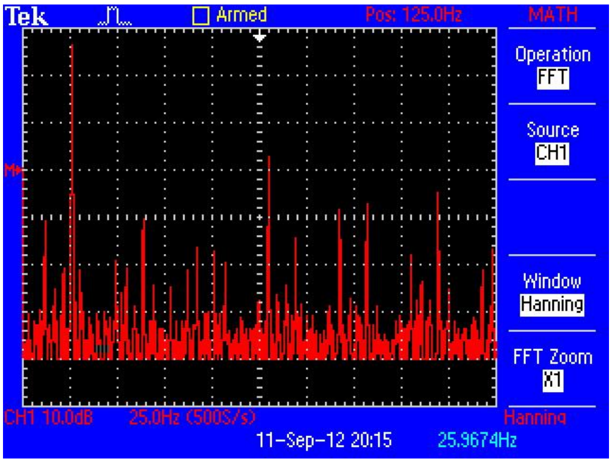

Fig.26: Fourier series of phase 1- voltage curve @ 360 rpm, medium generator

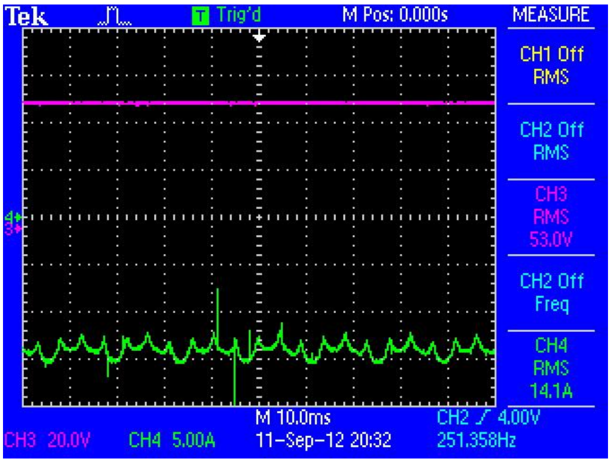

Fig.27: Rectified voltage and current @ 360 rpm, medium generator

Fig.27 visualizes the rectified DC-voltage (purple) and -current (green) on the oscilloscope. In this situation, the battery voltage is 53V while strong 14.1A are recharging the batteries at rated power.

5.) The power-drop in the bridge rectifiers can be appreciated when comparing the AC- to the DC-efficiency under battery-connection.

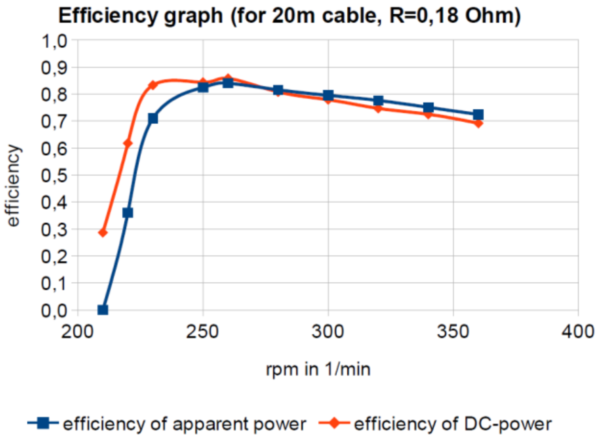

Graph 12: Comparing efficiencies for R_{cable}=0,18 Ohm, medium generator

Battery-connected, both efficiencies are visibly lower than 90%, going down to 70% close to rated power. This is a significant decrease compared to the efficiencies under ohmic load (no batteries) according to Test 2.

The higher the resistance, the later (higher) the cut-in rpm can be detected, since less current is flowing. Before cut-in, when I_{DC} = 0A and $V_{DC} < V_{Batt}$, the DC- shows higher values than the AC-efficiency. This is physically impossible and goes back to the effect of the constant open circuit battery voltage. After the cut-in, the differences between the two curves resemble the additional losses within the AC/DC rectification process.

6.) The overall efficiency between driving force down to the batteries is expressed by the DC-efficiency, which is significantly lower compared to the AC-efficiency of the previous Test 2. However, certain end-of-line-losses, such as internal battery- or inverter- losses are still not represented even in the following graph.

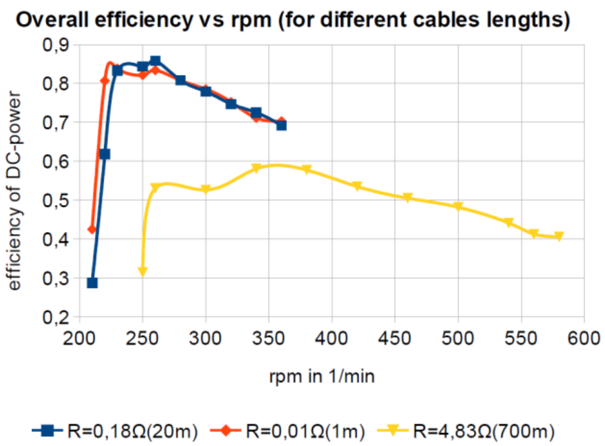

Graph 13: Overall DC- efficiency for all cable resistances

All scenarios have their best efficiency point shortly after cut-in rpm. As the current-flow increases, the DC-efficiency begins to suffer, mainly due to higher heat losses in the system.

4.6 Test 6: Battery connection and additional load (medium generator)

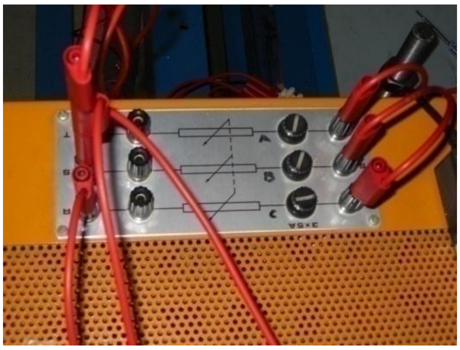

Photo 11, Test 6, battery connection and additional load

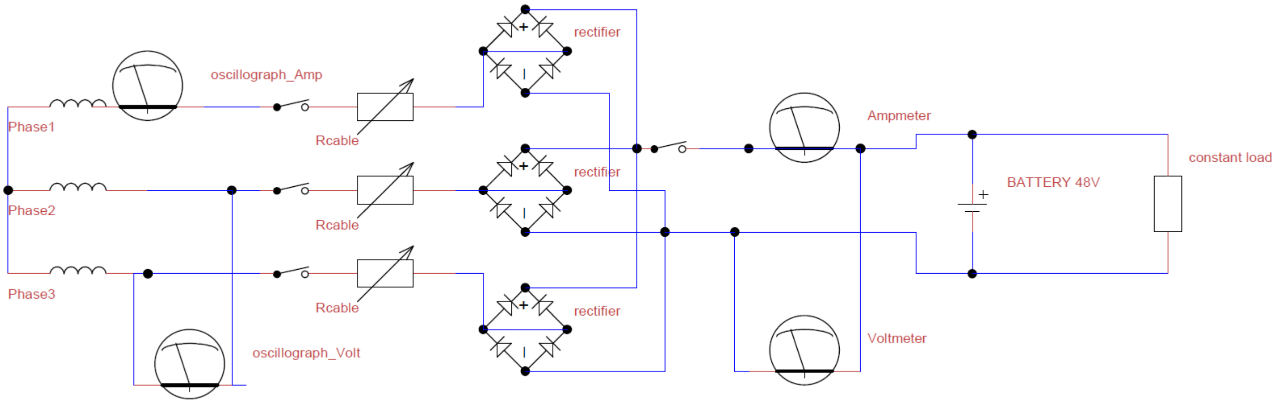

Fig.28: Set-up for Test 6

Set-up: The set-up is similar to previous Test 5. The **medium generator** is connected to the battery bank with the 20 meter long cables: R_{cable} = 0.18 Ohm. Additionally, a considerable load of R = 3.73 Ohm is connected to the batteries, allowing for $I_{load} \approx$ 14A = constant to be dissipated permanently.

Purpose: Analysing the performance of the medium generator at different rpm and constant cable resistance, connected to a battery bank as well as a 'heavy' additional ohmic load, in terms of battery current/voltage, efficiency and frequency-distribution. Comparing the performance of the system with and without additional load.

Instruments: Oscilloscope, torque meter and multi-meter.

Summary of results:

- The batteries sustain the load with current, stabilizing the system. As rpm increase, the generator relieves the batteries increasingly from the load.

- The battery-voltage determines the performance of the system: an additional load, resembling electricity consumption, results in lower voltage levels and consequently higher current flows.

- When defining the best cable resistance, the crucial impact of the battery voltage must be considered, too.

Results in detail:

1.) Since R_{load} = 3.73 Ω = constant ⟶ $\mathrm{I_{load}} \approx 14\ \mathrm{A} = \mathrm{const.}$

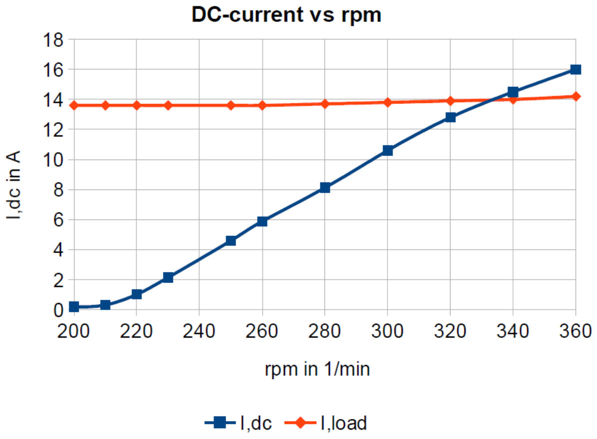

Graph 14: Current coming from the generator (blue) and going into the load (red), medium generator

The difference between the current coming from the generator and going into the load is provided by the batteries ΔI = I_{load} - I_{DC}. As I_{DC} rises with rpm, the batteries are more and more relieved from the load, until at rpm = 340 $\frac{1}{\mathrm{min}}$, the load is sustained entirely by the generator.

The load resembles constant electricity consumption, making Test 6 a realistic scenario for a wind powered battery system, where rpm increases with wind speed. Until there is enough wind power available, it is mainly the stored energy in the batteries, which satisfy and stabilize the consumption. It is for this reason that electrical systems need to be stabilized by storage- and back-up-systems, e.g. batteries.

2.) The load dissipates $P_{load} \approx 650W = constant$, simulating the use of low-powered devices such as lights, music, fridge and computers, etc. An additional load influences the performance of the system visibly.

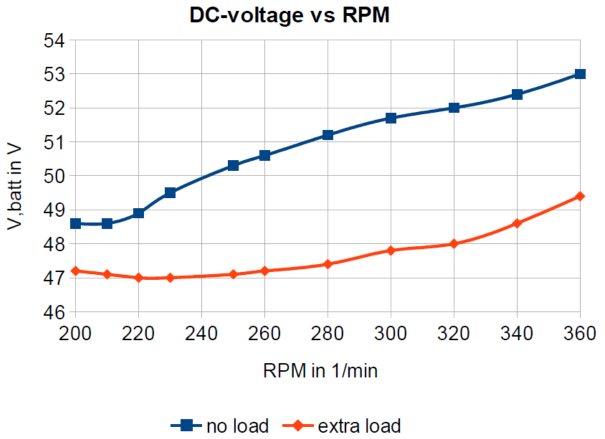

Graph 15: Battery-voltage in relation to rpm, with and without extra load, medium generator

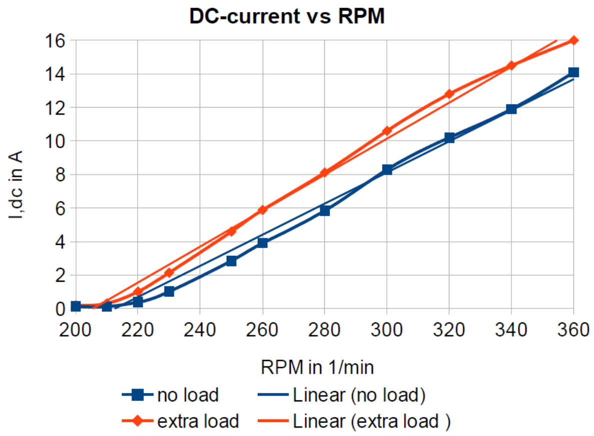

Graph 16: Current in relation to rpm, with and without extra load, medium generator

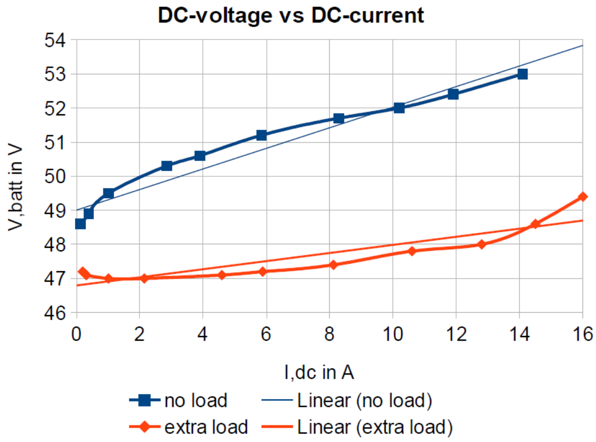

Graph 17: Direct relation between current-flow of generator and battery-voltage with and without extra load, medium generator

The above graphs visualize the very importance of the battery voltage on the overall system performance. In the same way that high currents (consumption) provoke the voltage to drop, low battery voltage (empty batteries) result in higher currents, too. As proven in Test 2, current is analogue to torque, which is a crucial factor in terms of the rotor blades' performance and thus the efficiency of the whole system. When defining an appropriate cable resistance (Test 7), the impact of the battery voltage must be considered.

It can be noted that at low rpm, when the generator is hardly contributing to providing the high load current, the battery-voltage drops down to $V_{batt} \approx 47V$. This comes close to a dangerously low voltage since $V_{batt,single} \approx 11.75V$.

3.) According to Graph 18, the DC-efficiency is also affected by the battery voltage, i.e. additional load.

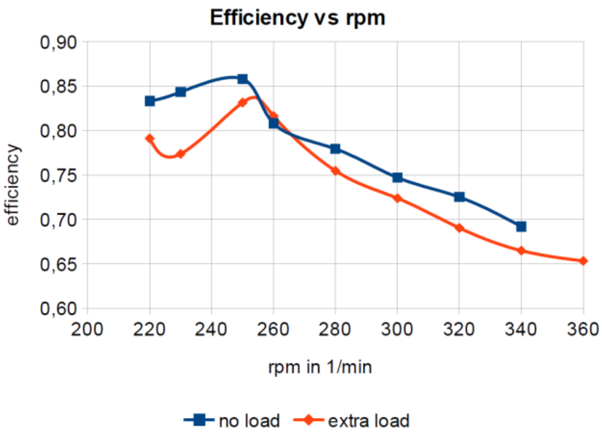

Graph 18: Comparison of DC-efficiency with and without extra load, medium generator

- Higher current-flow means more torque, i.e. more relative mechanical power and thus less DC-efficiency.

- Higher current-flow means more heat losses, i.e. less relative DC-power and thus less DC-efficiency.

The additional drop in DC-efficiency due to a strong extra load amounts up to approximately 3%.

4.) By changing the set-up of the experiment and **varying the load-resistance** while keeping **rpm = const. = 260 $\frac{1}{\min}$** the previous results are confirmed: the battery voltage decreases as the load-current increases at rpm = const.

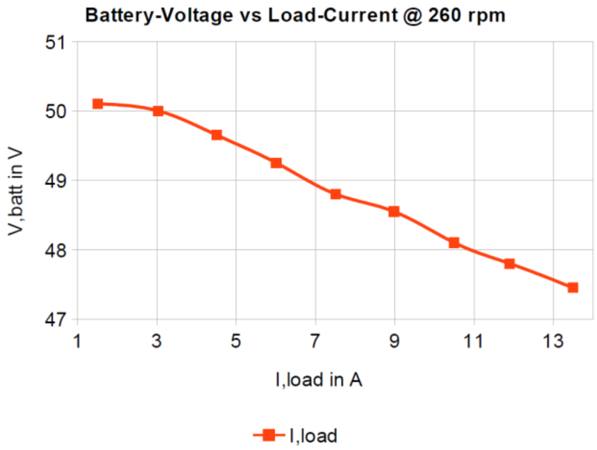

Graph 19: Battery voltage vs. load-current at constant rpm, medium generator

5.) The wave form as well as the fourier series look very similar to previous Test 5 and will therefore not be repeated at this point.

4.7 Test 7: The interaction between generator and rotor blades under battery connection

Set-up: The power curves for different cable resistances of the **battery-connected medium size generator** (Test 5 and 6) are combined with the power field simulation of its corresponding rotor blades.

Purpose: Analysing the interaction between generator and rotor blades, in order to maximise the overall efficiency of a complete wind turbine system.

Instruments: The open source simulation programme Oblade[4] for rotor blades of wind turbines, developed by the Technical University (TU) of Berlin.

Summary of results:

- In order to get an overview of the interaction between the performance of generator and rotor blades, the power curves of the medium generator (Test 5 and 6) have to be combined with the simulated power field of exactly the corresponding blades.

- Both cable resistance and battery voltage are the main variables which determine the efficiency (good or bad interaction) of a given wind turbine at variable operating points.

- Very high cable resistances lead to significant losses in lower wind speeds, very low cable resistances in higher wind speeds. There are three general possibilities to regulate the system by means of the cable resistance:

---

[4] http://qblade.de.to/

- Simple solution: defining the most appropriate constant cable resistance.

- Middle way: a simple two gear system, adjusting the resistance value of the cable resistance.

- Advanced solution: permanent MPP- tracking system, fine-tuning the value of the cable resistance automatically and at all times.

Results in detail:

1.) Firstly, a power-field simulation of the rotor blades needs to be developed with Qblade. For this matter, both profile and blade geometry of the wooden blades (chord, angle of attack, etc.) have to be measured precisely and fed into the programme. The generated data can be prepared with common programmes such as Excel or Open Office Calculator in order to visualize the mechanical power generated by the rotor blades, for a variety of windspeed/rpm- combinations.

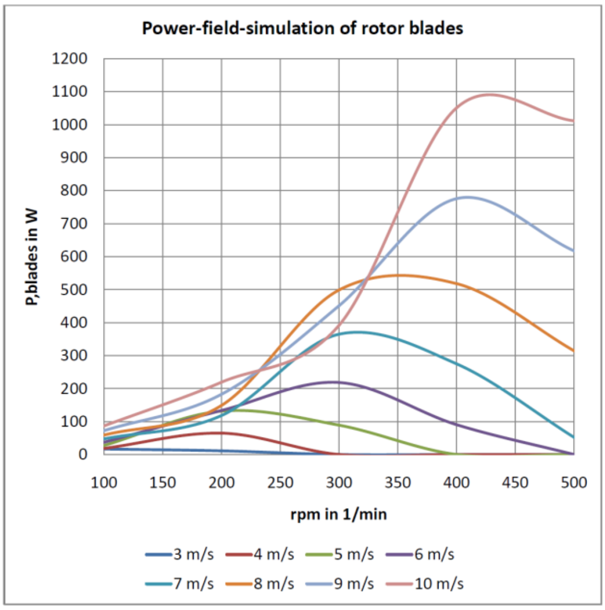

Graph 20: Power-field-simulation of corresponding rotor blades, medium generator

As expected, the lower the wind speeds, the lower the rpm which is appropriate for an efficient mechanical power generation of the blades and vice versa.

2.) In order to get an overview of the interaction between generator and rotor blades, the power curves of the medium generator (Test 5) are combined with the power field of the corresponding blades.

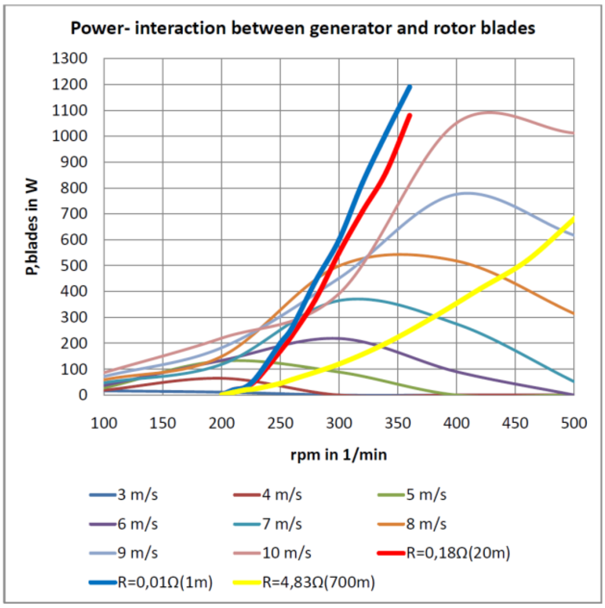

Graph 21: Power field of rotor blades meets power curves, medium generator

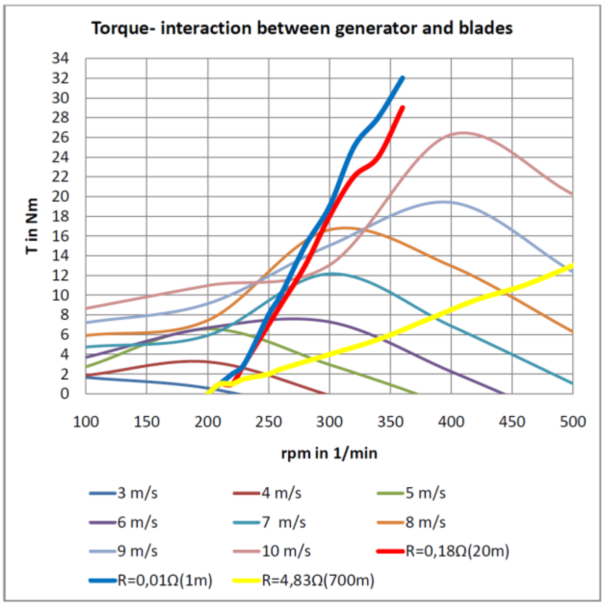

Graph 22: Torque field of rotor blades meets torque curves, medium generator

Graph 21 represents a very user-friendly overview of the compatibility between generator and rotor blades: an efficient performance is given, when the power curves of the generator cross the peaks of the respective rotor blade field. The conclusions that can be drawn from the above graphs are:

- Very high cable resistance values result in poor efficiency at all wind speeds, since there is a big offset between the generator curve and the peaks of the different blade curves. It must be pointed out that R_{cable}=4,83 Ω is anyhow not realistic, since it is the equivalent of more than 700 meters of a 3-phase-cable at $\mathrm{A_{cable}} = 2{,}5\ \mathrm{mm}^2$.

- Low cable resistance values result in relatively good efficiencies for lower wind speeds up to 8 m/s, but inhibit the blades to reach rated power. In fact, for v_{wind} > 8m/s and due to the steep increase in torque, the rotor blades start stalling: $rpm \leq 300\ \frac{1}{min}$. The maximum mechanical power is then only around 500 W, which is nowhere close to $P_{DC,rated}$ = 850W. The steeply increasing amount of energy in high winds cannot be extracted. It is important to note, that the predominant wind speeds for small scale installations is realistically in the range of 3 m/s < v_{wind} < 7 m/s, where efficient performance is most important. On the other hand, since $P_{Wind} \sim v_{Wind}^3$, inefficiency in high winds due to stall can reduce the overall energy expectancy by a good deal, particularly at sites with high winds.

3.) The results so far have kept the impact of the battery voltage unattended. Following from Test 6, the battery voltage depends both on the amount of additional load on the system (consumption) and the batteries' state of charge. Under P_{load} ≈ 650W (Test 6), the power curve of the generator changes visibly for a given constant **cable length, here R = 0,18 Ω = const.**

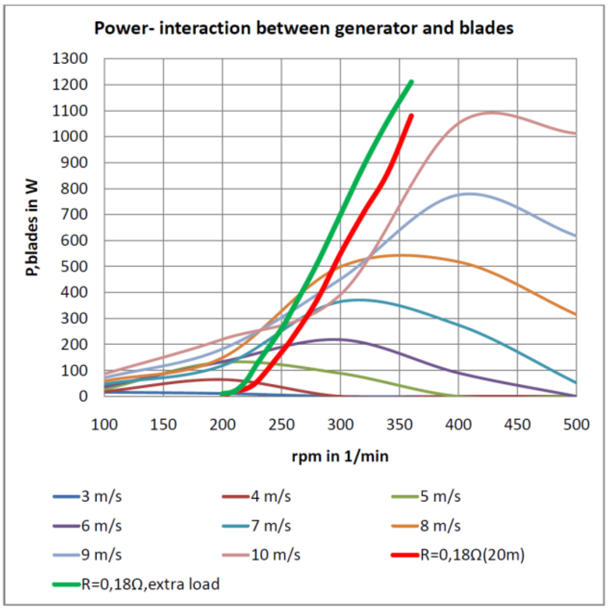

Graph 23 : Power field of rotor blades meets power curves with and without additional load, medium generator

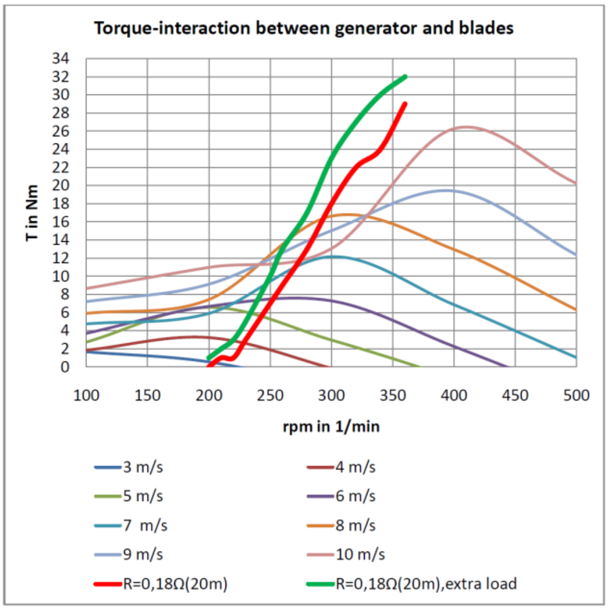

Graph 24: Torque field of rotor blades meets torque curves with and without additional load, medium generator

Connecting the additional load to the batteries, the rotor blades start stalling already at rpm ≈ $275\frac{1}{\mathrm{min}}$, which is immediately after the cut-in of $rpm_{cut\text{-}in} \approx 225\frac{1}{\mathrm{min}}$, allowing for a power generation of no more than P_M= 400W (green curve). In fact, for v_W > 8 m/s less power can be extracted than for v_w = 8m/s. This situation is comparable to cycling uphill by bike in the highest (hardest) gear possible.

Looking at the whole system, low battery voltage is critical and requires most efficiency: either the batteries' state of charge is low or a strong additional load needs to be sustained. As a result, it is thus the steeper, i.e. loaded power curve (green) which must be considered when defining the most appropriate cable resistance. It is in these situations that the batteries need the most effective support possible from the generator!

4.) Neither of the three cables used in Test 5 and 6 are appropriate or realistic for wind turbine installations. The AC- cables from the top of the tower will in most cases be longer than 20m, but considerably shorter than 700m (at $\mathrm{A_{cable}} = 2{,}5\ \mathrm{mm}^2$), until they reach the object that needs to be powered, unless the electronics are put into a secure box right on the bottom of the tower.

The curves for (realistic) cable lengths higher than 20 meters at A_{cable}= 2.5mm^2 are increasingly shallow in comparison to the ones shown in Graph 23 and 24, which, conveniently enough, makes them more appropriate in terms of the overall system performance.

All following strategies for improved performance between generator and rotor blades are based on these assumptions:

- The AFPM generator is battery-connected.

- The system runs torque-free (on open circuit) before cut-in for $v_W \leq 3m/s \longrightarrow$ $V_{DC} < V_{Batt}$ and I_{DC} = 0A.

- The rotor blades include a mechanical furling system which determines $P_{rated} \leq 850W$ for v_W >10m/s.

5.) The simple solution: defining the most appropriate **constant** cable resistance:

a) The battery voltage should be assumed critically low, between 11,5V < $V_{Batt,single}$ < 12V. The very reason for the batteries being low can be due to additional load (consumption) or shallow state of charge, both of which are critical situations before the system shuts down: The efficiency must be as high as possible.

b) The cable resistance should allow for ideal efficiencies in low wind speeds of 3m/s < v_{Wind} < 7m/s, since tower heights under 15 meters generally offer poor wind speeds.

c) The cable resistance should allow for $P_{DC,rated} \approx 850W$ to be reached, without the blades stalling, i.e. the power curve should cross the wind curve for 9m/s < v_{Wind} < 10m/s somewhere close to $P_M \approx 1000W$(depending on η_{DC}).

Cable resistances, which fulfil these conditions and for **this specific set-up** are assumed to be in the range of $0{,}3\Omega < R_{cable} < 0{,}6\Omega$. For precise values, more experiments are required.

6.) The middle way: a simple two gear system, adjusting the cable resistance:

Older concepts of **a**synchronous wind turbine generators function with a two gear system, by activating or deactivating additional pole-pairs (Test 1). In this way, the torque/rpm relation can be adapted for lower and higher wind-speeds in order to reach higher efficiencies.

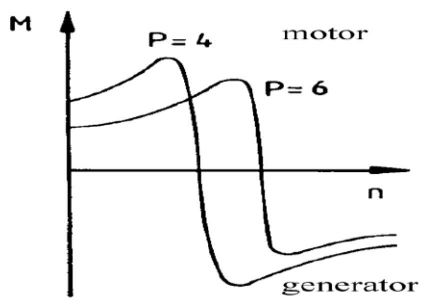

Fig. 29 The concept of a pole-pair-regulated asynchronous motor/generator (where M is torque and n is rpm)

Here, a simple wind speed monitoring system would be able to switch between cable resistances (gears) for low and high winds. The low gear (high resistance) could be realized by adding an appropriate additional resistance R_{series} in series to R_{cable}, so that the modified resistance is $R_{mod} = R_{cable}+R_{add}$, which could be de-/activated by a simple relay. In this way, the green curve of Graph 31 would be switched at $v_{switch} \approx 7m/s$ to a smoother curve, allowing the rotor blades to reach rated power.

For a precise layout of such a system, a proper design and more tests are required.

7.) Advanced solution: permanent MPP (Maximum Power Point)- tracking system:

These systems, which are by now common as part of solar- and wind powered systems, are tracking down the best ratio between output voltage and current for each possible operational point. Technically, this is achieved by manipulating the resistances, thus current-flow, accordingly.

For a precise layout of such a system, a proper design and more tests are required.

5 SUMMARY

The presented test-results show that

- Axial Flux Permanent Magnet (AFPM) Generators have a high potential due to their

  - simple and robust design.

  - high efficiency, both grid- and battery- connected.

- The interaction between the generator and its rotor blades need to be fine-tuned in order to obtain high efficiencies for a wide range of operating points (wind speeds), depending on:

  - the ohmic cable resistance between generator and batteries.

  - the battery-voltage, i.e. their state of charge and the additional load (consumption).

By having analysed AFPM generators in all detail, this measuring campaign contributes to

- Further research regarding the appropriate use of such generators particularly within renewable energy systems.
- The development of a reliable and efficient measuring campaign in order to check and improve the quality and safety of such generators.
- The design and realization of educational courses, particularly laboratory courses in technical universities and institutes.
- The breakthrough of Open Source Hardware in the renewable energy sector.

6 REFERENCES

[Piggott]:

Piggott, Hugh: *A Wind Turbine Recipe Book*. Scoraig, 2009.

[Latoufis]:

K. Latoufis, G. Messinis, P. Kotsampopoulos, N. Hatziargyriou: *Axial flux permanent magnet generator design for low cost manufacturing of small wind turbines*, Wind Engineering, Volume 36, No. 4, 2012.

Further references, which have indirectly contributed to this report:

- Piggott, Hugh: *Wind Power Workshop*. Machynlleth (UK): CAT Publications, 2011.
- Wind Turbines-Part2: Design Requirements for Small Wind Turbines, CEI/IEC Std. 61400-2, 2006.
- “Microgrids”, Hatziargyriou, N.; IEEE Power and Energy Magazine, Volume 6, Issue 3, May-June 2008 Page(s):26 – 29 (2011)
- The Practical Action website. [Online]. Available: http://practicalaction.org/
- Bartmann D., Fink D., Homebrew Wind Power: Hands-on guide to harnessing the wind, Buckville Publications, 2009.
- J. R. Bumby, N. Stanard, J. Dominy, and N. McLeod, “A Permanent Magnet Generator for Small Scale Wind and Water Turbines” in Proc. of the 2008 International Conference on Electrical Machines, paper 733, p. 1.
- A. Parviainen, J. Pyrhonen and P. Kontkanen, “Axial Flux Permanent Magnet Generator with Concentrated Winding for Small Wind Power Applications” in Proc. of the 2005 IEEE International Conference on Electric Machines and Drives, p. 1187.
- K. Latoufis, A. Gravas, G. Messinis, N. Korres, N. Hatziargyriou, “Locally manufactured open source hardware small wind turbines for sustainable rural electrification”, 3rd World Summit for Small Wind, 15-16 March 2012, Husum, Germany
- J.F. Gieras, RJ. Wang and MJ. Kamper, Axial Flux Permanent Magnet Brushless Machines, 2nd ed. Springer, 2008.

7 CONTACTS

Joerg Alber: joerg.alber@gmx.net

Kostas Latoufis: latoufis@power.ece.ntua.gr